



## Comparative Analysis on Isotherm and Kinetic Modelling for the Adsorption of Carcinogenic Pollutants onto Modified Graphite Intercalation Compounds (GICs)

F. Raza<sup>1</sup>, T. Ahmad<sup>1\*</sup>, H.M.A. Asghar<sup>2</sup>, M. Irfan<sup>3</sup>, H.A. Mannan<sup>4</sup>, A. Afzal<sup>1</sup>, Z.B. Babar<sup>1</sup>

Submitted: 04/08/2025, Accepted: 20/10/2025, Published 25/10/2025

### Abstract

Industrial, agricultural, and domestic activities have been generating various carcinogenic pollutants and imparting toxic, non biodegradable, and long-enduring impacts on both humans and animals, even at low concentrations. This article has been reported for the first time to investigate the kinetics and isotherms models of carcinogenic pollutants including Acid violet 17 (AV17), Mercaptan 1, Humic acid, Phenol and Methylene Blue (MB), which were adsorbed on the surface of NYEX® 1000. The effects of adsorbent dosage and contact time for AV 17 (8.2-70 ppm), contact time (0–180 min), Mercaptan 1 (11.7–100 ppm), contact time (0–180 min), Ethane Thiol (7.5-50 ppm), contact time (0–180 min), Humic acid (21.7-60 ppm), contact time (0–120 min), Phenol (8.8-70 ppm), contact time (0–180 min) and MB (11.7-100 ppm), contact time (0–180 min) were investigated against NYEX® 1000 respectively. The kinetics findings showed the adsorption of Humic acid ( $R^2=0.99908$ ), AV 17 ( $R^2=0.9977$ ), Mercaptan 1 ( $R^2=0.9982$ ), Phenol ( $R^2=0.9989$ ) and MB ( $R^2=0.9966$ ) on the surface of NYEX® 1000 were well described by Pseudo-second order kinetics. The Pseudo-1st order kinetics revealed lower regression coefficient values for all pollutants, confirming it to be least followed. The Isotherm models such as Halsey ( $R^2=0.9971$ ,  $R^2=0.9485$ ) showed the good agreement to describe the equilibrium of AV 17 and Phenol adsorption respectively. On the contrary, equilibrium adsorption of Mercaptan 1, Humic acid and MB on the surface of NYEX® 1000 was found to be well described by Dubinin-Radushkevich with  $R^2= 0.984$ ,  $0.9331$  and  $0.9766$  respectively. It would be undoubtedly valuable for achieving a comprehensive explanation of the adsorption process and ultimately enhancing the removal performance.

**Keywords:** Kinetic Modelling, Mercaptan, Phenol, Humic Acid, Methylene Blue

### 1. Introduction:

Pollution refers to harmful changes in the physical, chemical, or biological characteristics of air, water, and land, primarily caused by increase in human activity. Both the environment and human life have suffered as a result of this transformation, whether on purpose or accidentally. The composition of the Earth's soil, water, and air has changed in recent decades due to the discovery of several pollution-causing elements [1, 2].

Modernization, population growth, and urban development have all contributed to a significant rise in pollution and environmental deterioration on a global scale. While population growth has also presented several challenges, it has significantly contributed to water pollution. Increased urbanization has resulted in a higher concentration of people in limited spaces, leading to the expansion of buildings, roads, sewage and storm drains, vehicles, factories, urban waste, aerosols,

<sup>1</sup> Institute of Energy and Environmental Engineering, University of the Punjab, Lahore, Pakistan

<sup>2</sup> Institute of Chemical Engineering & Technology, University of the Punjab, Lahore, Pakistan

<sup>3</sup> Pakistan Council of Scientific and Industrial Research, Lahore, Pakistan

<sup>4</sup> Institute of Polymer and Textile Engineering (IPTE), University of the Punjab, Lahore, Pakistan

\*Corresponding Author: Tausif Ahmad ([tausif.ieee@pu.edu.pk](mailto:tausif.ieee@pu.edu.pk))

smoke, ash and dust. These factors collectively have a negative impact on the environment, exacerbating several ecological issues [3-5]. Various synthetic chemicals used as fertilizers and pesticides, along with toxic substances in industrial sewage, are carried into rivers and lakes through surface runoff, especially during rainfall. Additionally, these contaminants infiltrate the soil and percolate into groundwater. Commercial and industrial wastes constitute a significant portion of solid waste. The introduction of various synthetic chemicals into aquatic environments results from multiple sources, including natural processes, Industrial waste (chemical production facilities, petrochemical, paper industries, textile and paint industries), and agricultural activities. Textile industries discharge large volumes of hazardous wastewater, which poses serious risks to the environment. The liquid effluent is generated by the textile and leather industries often contains significant amounts of dyes, contributing to water pollution. Exposure to these textile dyes can also cause various health issues for humans, including congenital malformations, skin irritations, respiratory problems, nausea, and headaches [6-8].

Recent research indicates that azo dyes are being widely employed in several industrial sectors, including textile, food, and cosmetics industries and have the potential to be harmful to human health and the environment due to their carcinogenic, poisonous, and allergic properties [9, 10]. Study have suggested that AV 17 may have harmful effects, including carcinogenic, allergic and toxic impacts, particularly when released uncontrollably into the environment [11, 12]. Phenol and phenolic compounds are widespread pollutants that enter natural water sources through the effluents of various chemical industries, including coal refineries, resin production, petrochemical, paint, textile, dyeing, pharmaceuticals and pulp mills. These toxic compounds exhibit physiological as well as genotoxic, immunotoxin, hematological and carcinogenic associated features. They hold a high bioaccumulation tendency rate within the food chain due to their lipophilic nature, ultimately creating severe environmental concerns [13, 14]. Additionally, mercaptan, a significant intermediate in organophosphorus pesticide production, poses severe environmental and health risks, such as causing CNS damage, headaches, nausea, and even fatal respiratory paralysis, a life-threatening condition that may result in death [15, 16]. The discharge of untreated effluents

containing humic substances such as humic acid into freshwater bodies presents a genuine environmental threat, potentially leading to toxic by-products and contamination [17, 18]. Organic contaminants in water can significantly alter its aroma, color, and taste, and they interact with chlorine during treatment processes, leading to the creation of disinfection by-products (DBPs) associated with serious health hazards [19-21]. Textile producers regularly discharge MB dyes into natural water sources, jeopardizing both human and microbial health. MB dye poses a health threat to humans at elevated concentrations due to its considerable toxicity [22]. Besides being non-biodegradable, toxic, and carcinogenic, MB can also adversely affect the environment and significantly threaten human health [23]. Visual impairments, behavioral and gastrointestinal difficulties, respiratory complications, and abdominal infections are among the health hazards linked to MB. Besides inducing skin and ocular irritations and the demise of immature cells in tissues, it also leads to methemoglobinemia, tissue necrosis, nausea, vomiting, diarrhea, cyanosis, shock, gastritis, jaundice, and tachycardia [24]. The effective removal of organic pollutants from wastewater is crucial for safeguarding human health and ecological systems due to their high toxicity, structural durability, and prolonged environmental persistence. Conventional biological treatment methods frequently inadequately address these contaminants because of their limited biodegradability. As a result, more advanced physical and chemical treatment techniques are utilized to mitigate high concentrations of organic pollutants. Traditional techniques, such as membrane filtration, ion exchange, ozonation, and Fenton oxidation possess notable qualities, including high purity, selectivity, and efficient separation of precious metals. Nevertheless, several operational challenges, complex equipment, high costs, and the use of hazardous chemicals remain considerable obstacles to their widespread adoption [25, 26]. Traditional biological treatment processes frequently prove inadequate in addressing specific pollutants due to their low biodegradability. Consequently, more sophisticated physical and chemical treatment methods are utilized to address elevated levels of organic pollutants. Conventional methods such as membrane filtration, ion exchange, ozonation, and Fenton oxidation have remarkable attributes, including elevated purity, selectivity, and

effective separation of precious metals. However, numerous operational hurdles, intricate gear, substantial prices, and the utilization of dangerous chemicals persist as significant barriers to their extensive implementation [27-29]. Isotherm and kinetic models are essential for elucidating the equilibrium relationship between the reduction of pollutant concentration in solution, optimizing adsorbent performance, and enhancing treatment efficiency. Kinetic models emphasize the rate and mechanism of the adsorption process, while isotherm models concentrate on the link between the quantity of adsorbate adsorbed onto the surface and its concentration in solution.

The adsorption process is widely accepted for removing both organic and inorganic contaminants. It is particularly effective in reducing organic contaminant concentrations to acceptable levels compared to other conventional treatment techniques. Additionally, adsorption is a fast, reliable, and cost-effective decontamination technique [30-32]. However, the full potential of adsorption can only be achieved through investigations of its various facets, such as adsorption kinetics and isotherms. To help scientists better describe adsorption dynamics and equilibrium, mathematical formulas known as adsorption isotherms can be used to interpret adsorption equilibria [33]. To understand adsorption dynamics, improve adsorbent performance, and create efficient treatment systems, it is crucial to utilize isotherm, and kinetic models are essential in adsorption-based pollutant removal. Kinetic models concentrate on the rate of adsorption and mass transfer, whereas isotherm models explain the equilibrium relationship between the concentration of the adsorbate and the amount adsorbed. Therefore, research on isotherm and kinetic modelling hold an insensible importance for enhancing and optimizing the adsorption process along with operational design in removal of carcinogenic pollutants.

In recent years, Brown has explored an alternative adsorption method using a novel, nonporous, highly conductive graphite adsorbent substance known as NYEX® 1000. It has been reported; this adsorbent can be regenerated quickly and with minimal consumption of energy [34-36]. The NYEX® 1000 has been efficiently deployed for the electrochemical removal of AV17, Mercaptan 1, Humic acid, Phenol and MB [37].

However, Isotherm and Kinetic modelling based investigation via employing pseudo-first-order [38] and pseudo-second-order models [39] along with adsorption isotherms—including Temkin, Dubinin-Radushkevich, Halsey, Harkin-Jura, Jovanovic, and Elovich isotherms has been conducted for the first time for obtaining a comprehensive explanation of the adsorption process. The approach to isotherm modeling varies, leading to differences in the physical and chemical interpretation of model parameters. This paper is focused on adsorption isotherms and kinetic modelling of various organic pollutants onto the NYEX® 1000 as an adsorbent, considering initial concentration and stirring time as key variables

## 2. Material and methods:

### 2.1. Adsorbent:

In the current study, NYEX® 1000 (95 wt% carbon and featuring particle diameters ranging between 100 and 700  $\mu\text{m}$ ) has been employed as an adsorbent, a graphite intercalation compound (GIC) provided by Arvia Technology Ltd. The material contained 1  $\text{m}^2/\text{g}$  BET surface area, which was notably lower as compared to commercially available activated carbon. Additionally, NYEX® 1000 has also demonstrated an electrical conductivity of approximately  $0.16 \Omega^{-1}\text{cm}^{-1}$ , which has made it a unique adsorbent for the research conducted [37].

### 2.2. Adsorption Study:

The removal of carcinogenic pollutants was conducted through a batch process at ambient conditions to assess the adsorption kinetics and determine the process rate. This involved examining the effect of varying pollutant concentrations, and establishing the time needed to achieve adsorption equilibrium. A measured quantity of adsorbent was introduced into a defined volume of pollutant solution and continuously agitated using a magnetic stirrer at constant rpm until equilibrium was attained. At specific time intervals ( $t$ ), samples were periodically collected, passed through a micro-membrane filter and analyzed using UV-visible spectrophotometer at the pollutant's maximum wavelength (nm) to determine the solution concentration [37]. The adsorption capacity of the adsorbent at equilibrium was then determined using the appropriate equation.

$$q_e = (C_o - C_e) * V/m \quad (1)$$

Where  $C_e$  (mg L<sup>-1</sup>) denotes the concentration at equilibrium and  $C_0$  (mg L<sup>-1</sup>) denotes the adsorbate's initial concentration in the solution. The mass of the adsorbent added to the solution is denoted by  $m$  (g), whereas  $V$  (mL) represents the volume of the adsorbate.

### 2.3. Kinetic Modelling:

The evaluation of adsorption kinetics was conducted through experimental procedures involving specific concentrations of pollutants. A predetermined amount of adsorbent was added to the solution to ascertain equilibrium time. The mixtures were stirred with a magnetic stirrer at a specified rpm, samples were collected at regular time intervals, and the adsorbent was removed via micro-membrane filtering. The sample of specified concentration was analyzed using a UV-visible spectrophotometer to determine the maximum wavelength  $\lambda_{max}$  [37].

## 3. Results and Discussion:

### 3.1. Adsorption Kinetics:

Organic compounds utilizing the Arvia® method. Nyex® has been found, an efficient material for the removal and destruction of harmful and non-biodegradable substances with a strong electrical conductivity, derived from graphite intercalation. This adsorbent material is purported to be the first capable of straightforward, rapid, and economical electrochemical regeneration, a critical attribute that enhances the cost-effectiveness of the process. Nyex® has undergone assessment in laboratory-scale batch and continuous pilot plant experiments for the elimination of various organic pollutants. The procedure reportedly resulted in minimal material loss when conducted across numerous regeneration cycles. The substance was determined to be effective for the elimination of trace amounts of organic contaminants at a reasonable cost [37]. Kinetic studies are essential for understanding the dynamic behavior of adsorption, including time-dependent variations, transitory characteristics, and rate-limiting mechanisms. The results of this study provide essential criteria for the design and optimization of adsorption-driven treatment systems. The evaluation of the removal efficiency of diverse industrial pollutants encompasses several critical characteristics, including the adsorption rate, the initial concentration of the solute, and the loading capacity of adsorbent. These factors are all regulated by the physiochemical

properties of the adsorbent, including specific surface area, porosity, and surface chemistry. Furthermore, temporal measurement of adsorption is a crucial element of adsorbent efficacy. Kinetic models, such as pseudo first order and pseudo second order, were utilized and analyzed to choose the most suitable models for the experimental data [40]. The equilibrium time required for the adsorption of different pollutants was calculated, as shown above in **Figure 1**.

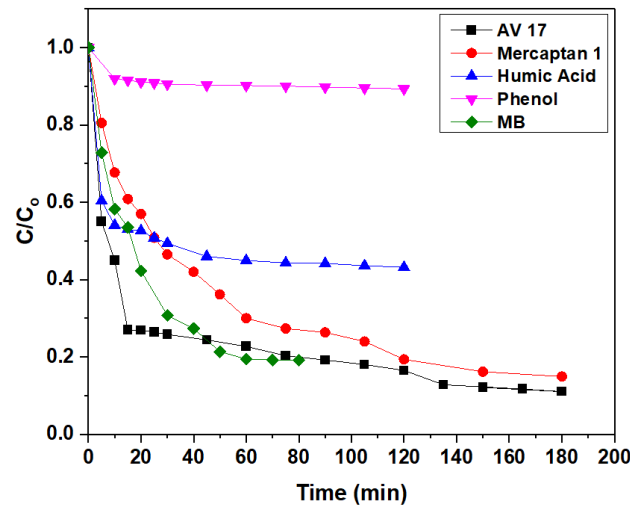


**Figure 1:** The kinetics of different waste water pollutants onto NYEX® 1000 adsorbent

### 3.1.1. Adsorption Kinetics Models:

The linearized form of pseudo 1<sup>st</sup> order rate kinetic model of Lagergren that based on solid capacity for sorption analysis is given by equation [41].

$$\ln (q_e - q_t) = \ln q_e - K_1 t \quad (2)$$

In this model,  $q_e$  and  $q_t$  (expressed in mg g<sup>-1</sup>) represent the quantity of adsorbate, adsorbed onto adsorbent at equilibrium and at any contact time  $t$  (min) respectively, and  $k_1$  (min<sup>-1</sup>) denote rate constant with the pseudo 1<sup>st</sup> order kinetics model. The pseudo 2<sup>nd</sup> order rate kinetic model that based on the sorption equilibrium capacity, and its linearized form is expressed by the following equation.

$$\frac{t}{q_t} = \frac{1}{(K_2 q_e^2)} + \left( \frac{1}{K_2 q_e} \right) * t \quad (3)$$

where  $q_e$  (mg g<sup>-1</sup>) and  $q_t$  (mg g<sup>-1</sup>) represent the amounts of adsorbate adsorbed on unit mass of adsorbent at equilibrium and at any contact time  $t$  (min), respectively, and  $k_2$  (g mg<sup>-1</sup> min<sup>-1</sup>) denote rate constant with the pseudo 2<sup>nd</sup> order adsorption kinetics model.

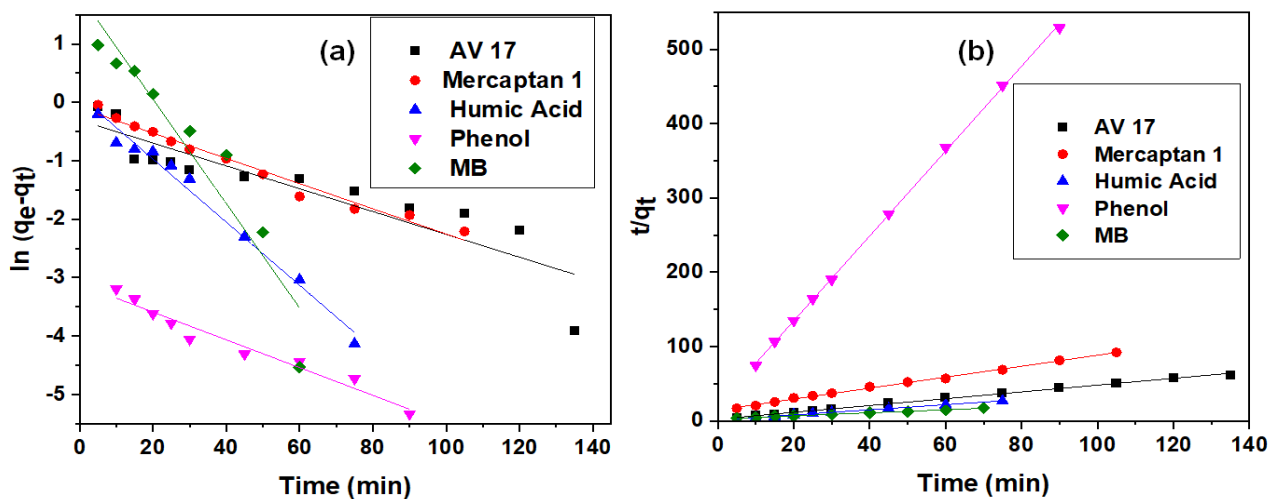


**Figure 2: (a)** Pseudo 1<sup>st</sup> order and **(b)** 2<sup>nd</sup> order kinetic models

The pseudo-first-order and pseudo-second-order adsorption models for different pollutants were calculated, as illustrated in **Figure 2**. It is clear from **Table 1** that greater efficiency of adsorption with initial concentration of pollutants, and then the initial concentrations of pollutants had no significant influence on the equilibrium time. The improved adsorption capacity of the adsorbent for a specific pollutant is likely, attributed to reduced diffusion resistance, a larger accessible surface area, and more robust adsorbate-adsorbent interactions.

**Table 1:** The characteristic values of the kinetics parameter of the models

Pollutants	Pseudo 1 <sup>st</sup> order kinetics			Pseudo 2 <sup>nd</sup> order kinetics		
	Kinetics Characteristic Parameters					
	q <sub>e</sub>	K <sub>1</sub> (min)	R <sup>2</sup>	q <sub>e</sub>	K <sub>2</sub> (g mg <sup>-1</sup> min <sup>-1</sup> )	R <sup>2</sup>
<b>AV 17</b>	1.024	0.027	0.764	2.271	0.061	0.9977
<b>Marcaptan 1</b>	0.973	0.024	0.969	1.426	0.031	0.9982
<b>Humic acid</b>	1.131	0.055	0.991	2.915	0.094	0.9997
<b>Phenol</b>	0.057	0.032	0.882	0.184	0.999	0.9989
<b>MB</b>	6.256	0.089	0.908	4.928	0.015	0.9966

The study employed two kinetic models, with all associated constants and correlation coefficients ( $R^2$ ) derived from their respective plots. The suitability of each adsorption model was evaluated by comparing key parameter values and the corresponding  $R^2$  values. The results demonstrated that the pseudo second-order kinetics provided a more accurate depiction than the pseudo first-order kinetic model. The elevated regression coefficient values ( $R^2 > 0.99$ ) for all contaminants validated the second-order kinetics with

the experimental results. It was determined that the pseudo second-order kinetic model provided a more precise and reliable representation of pollutant adsorption onto the NYEX® 1000 adsorbent than the pseudo first-order kinetic model. The result corroborated the experimental results and underscored the robustness of the pseudo second-order kinetics. The identification of the best suitable kinetic model for characterizing pollutant adsorption onto the adsorbent NYEX® 1000 was evaluated using  $R^2$  values, as displayed below.

### Pseudo 1<sup>st</sup> order kinetic model

### Pseudo 2<sup>nd</sup> order kinetic model

## Humic acid

## AV 17: Marcaptan

## 1: Phenol: MB

### 3.2 Adsorption Isotherm

The study of adsorption isotherms is essential for evaluating adsorbent capacity and enhancing overall adsorbent effectiveness.

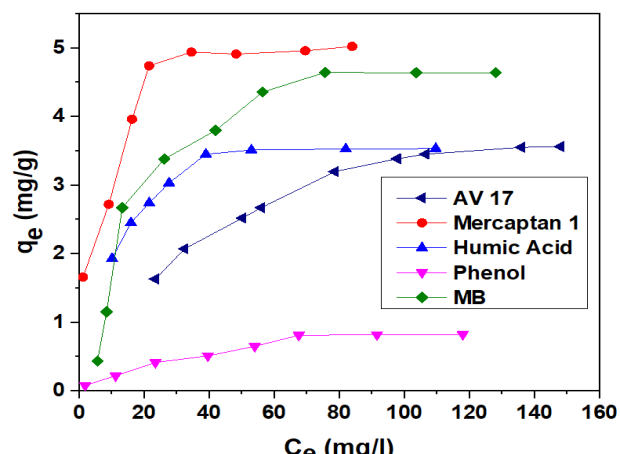


**Figure 3:** The Adsorption isotherms of different pollutants onto NYFX® 1000 adsorbent

Analyzing equilibrium adsorption capacity data is essential for interpreting experimental results and making accurate predictions. The adsorption capacity for various pollutants was determined via employing **Figure 3**. In this study, several adsorption isotherm models such as the Temkin, Dubinin-Radushkevich, Halsey, Harkin-Jura, Jovanovic, and Elovich isotherms were employed to evaluate the adsorption mechanism followed.

### 3.2.1. Adsorption Isotherm models:

Porosity and the mean free energy of adsorption were both estimated using the D-R (Dubinin-Radushkevich) isotherm adsorption model. The mean free energy value was indicated by either physical or chemical adsorption. The D-R isotherms model equation's linearized form is provided by

$$\ln q_e = \ln q_m - \beta \varepsilon^2 \quad (4)$$

Here,  $q_e$  (mg g<sup>-1</sup>) and  $q_m$  (mg g<sup>-1</sup>) represent the equilibrium adsorption capacity and the maximum amount of monolayer adsorption capacity on the adsorbent surface respectively. The activity coefficient is represented by the term  $\beta$  (mol<sup>2</sup> J<sup>-2</sup>), and the Polanyi potential, or  $\varepsilon$ , is used to get insight into the mean free energy  $E$  (kJ mol<sup>-1</sup>) of the adsorption process. The equation can be used to determine the  $\varepsilon$ .

$$\varepsilon = RT \ln \left( 1 + \frac{1}{C_e} \right) \quad (5)$$

Whereas  $R$  (J /mol K) and  $T$  (K) represent the universal gas constant and absolute temperature respectively. The mean free energy of adsorption process is following by

$$E = \frac{1}{\sqrt{2\beta}} \quad (6)$$

The Temkin isotherm adsorption model is more general, based on heat of adsorption. It considers that the heat of adsorption decreases linearly due to available coverage of all the molecules in layer on the adsorbent surface due to adsorbate-adsorbent interactions. It also assumes that the adsorption heat is constant across all binding sites by a homogeneous distribution of the binding energies up to some maximum binding energy. The linearized form of Temkin isotherm model equation is followed by

$$q_e = B \ln A + B \ln C_e \quad (7)$$

In this model,  $A$  (l mg<sup>-1</sup>) is the equilibrium binding coefficient, representing the maximum potential binding energy of the system, and parameter  $b$  serves as the Temkin isotherm constant associated with adsorption energy.

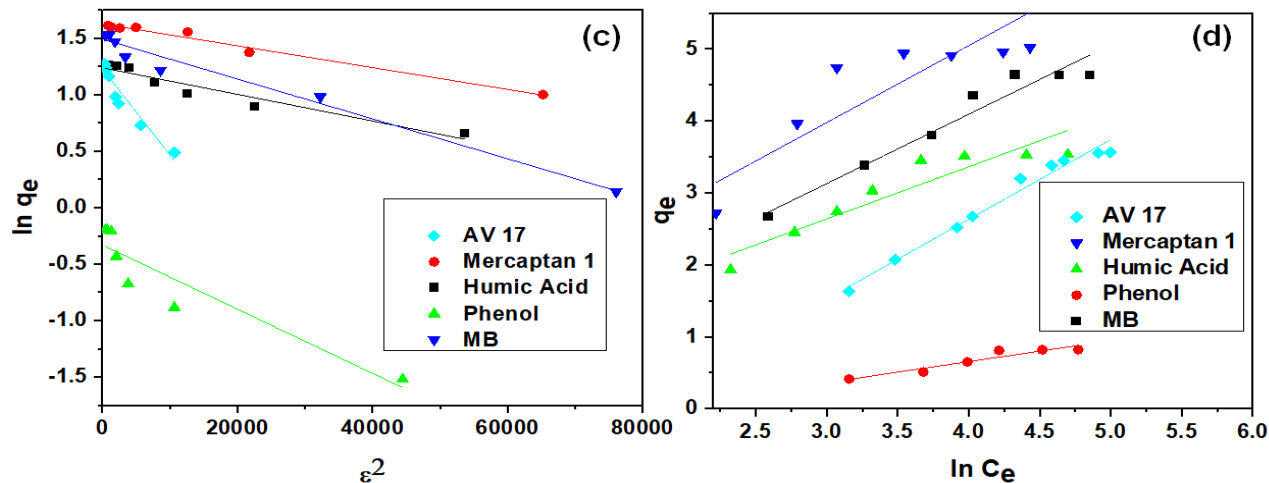


**Figure 4: (c)** The D-R isotherm and **(d)** Temkin isotherm adsorption model

Additionally,  $B$  (J mol<sup>-1</sup>) quantifies the adsorption enthalpy, which can be determined using the following relation

$$B = RT/b \quad (8)$$

Whereas all other parameters have the same meaning as in above model. The **Figure 4** illustrates the D-R and

Temkin isotherm models for adsorption of different pollutants. The adsorption isotherm constants for both models D-R isotherm and Temkin isotherm obtained from linear plot graph and the linear regression coefficient  $R^2$  for each evaluated condition are summarized in the Table 2.

**Table 2:** The parameter values of the D-R and Temkin Isotherm models.

Pollutants	D-R Isotherm model				Temkin Isotherms model			
	Isotherm Characteristic Parameters							
	q <sub>m</sub>	β(mol <sup>2</sup> J <sup>-2</sup> )	E(kJ mol <sup>-1</sup> )	R <sup>2</sup>	A(l mg <sup>-1</sup> )	B	B(J mol <sup>-1</sup> )	R <sup>2</sup>
AV 17	3.419	8E <sup>-5</sup>	0.077	0.9217	0.203	2261	1.096	0.9718
Mercaptan 1	5.090	1E <sup>-5</sup>	0.220	0.9840	4.125	2705	0.916	0.7466
Humic acid	3.453	1E <sup>-5</sup>	0.220	0.9331	2.347	3591	0.690	0.8617
Phenol	0.718	3E <sup>-5</sup>	0.130	0.8636	2.115	12265	0.202	0.9091
MB	4.410	2E <sup>-5</sup>	0.160	0.9766	0.306	1679	1.476	0.9496

The activity coefficient  $\beta$  that is used to find out the mean free energy gets for the range of D-R adsorption isotherm model from  $1E^{-5}$  to  $8E^{-5}$ , which strongly supports the validity in physical adsorption process. The values of mean free energy for all waste water pollutants are less than 8kJ/mol, describe the physisorption process. The Temkin isotherm constant values can be utilized to study the adsorption process associated with the heat changes of wastewater pollutants by NYEX® 1000 adsorbent. From the Table 03, it can be observed that the comparative study is significant with heat of adsorption which is governed by physical sorption process ( $R^2$ ) for adsorbent of different pollutants.

The correlation coefficient analysis indicated that the D-R isotherm model shows superior applicability for characterizing the adsorption process compared to the Temkin isotherm model. The Halsey isotherm model focuses on the multilayer adsorption mechanism on heterogeneous adsorbent surfaces, particularly in areas removed from the adsorbate-adsorbent interface. The linearized version of the Halsey isotherm is a valuable

instrument for analyzing adsorption mechanisms and surface phenomena.

$$\ln q_e = \left(\frac{1}{n_H}\right) * \ln K_H - \left(\frac{1}{n_H}\right) * \ln C_e \quad (9)$$

The constants  $n_H$  and  $K_H$  (mg g<sup>-1</sup>) in the equation denotes the adsorbent loading capacity and degree of heterogeneity on the adsorbent surface. Other symbols have same meant as in above models. These parameters offer a comprehensive understanding of the adsorption behavior in heterogeneous systems.

Harkin Jura Isotherm adsorption model is widely utilized for multilayer adsorption processes, particularly in systems where the adsorbent surface exhibits a heterogeneous pore distribution. Its application is particularly valuable in understanding the adsorption dynamics in porous and heterogeneous systems. The linearized form of equation is given by

$$\frac{1}{(q_e)^2} = \left(\frac{B_{HJ}}{A_{HJ}}\right) - \left(\frac{1}{A_{HJ}}\right) * \log C_e \quad (10)$$

while  $A_{HJ}$  (mg<sup>2</sup>/l) and  $B_{HJ}$  (mg<sup>2</sup>/l) denote the Harkin Jura isotherm parameters and other coefficients have same meaning as in above models.

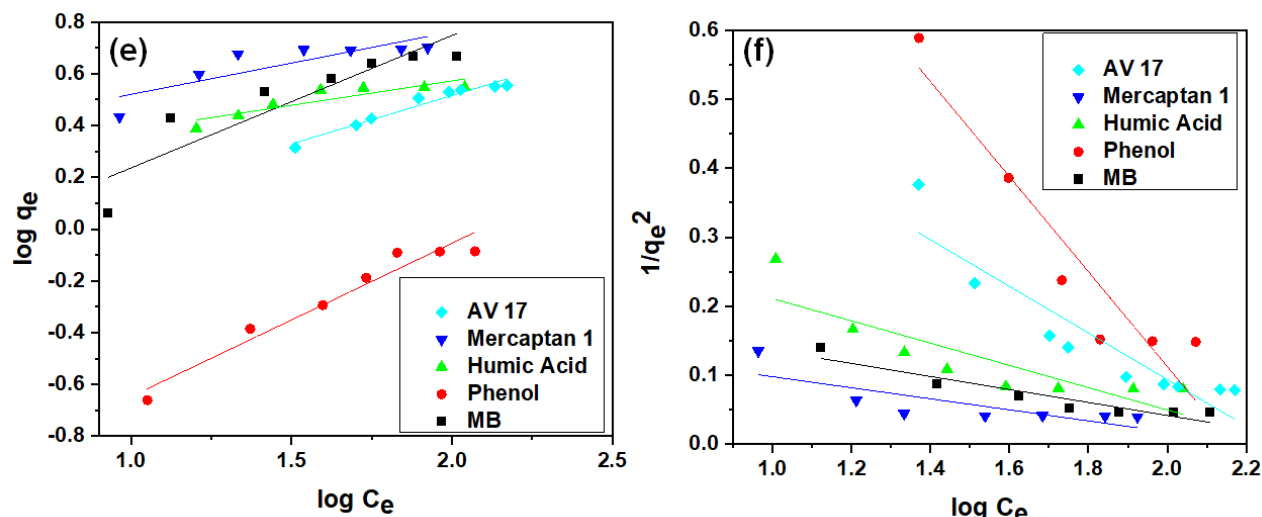
**Figure 5: (e)** The Halsey and **(f)** Harkin Jura isotherm adsorption model

Figure 5 presented the Halsey and Herkin Jura isotherm models applied, to describe the adsorption behavior for various pollutants. The parameter values of the Halsey isotherm and Harkin Jura isotherm models are calculated and presented in the Table. 3. The RC ( $R^2$ ) for both models indicated a relatively satisfactory fit, demonstrating their effectiveness in describing the adsorption behavior of the adsorbent. These results demonstrate the applicability of both isotherm models in analyzing the adsorption process under the observed conditions.

**Table 3:** The characteristic values of the parameter of the isotherm models

Pollutants	Halsey Isotherm model		Harkin Jura Isotherm model			
	K <sub>H</sub>	n <sub>Hj</sub>	R <sup>2</sup>	A <sub>HJ</sub>	B <sub>HJ</sub>	R <sup>2</sup>
AV 17	5.370	-4.230	0.9971	3.020	2.290	0.8461
Marcaptan 1	0.060	-4.230	0.7091	12.500	2.220	0.6292
Humic acid	0.090	-5.340	0.8001	6.250	2.320	0.7382
Phenol	2.510	-1.710	0.9485	1.510	2.180	0.8834
MB	3.160	-2.030	0.8199	3.220	2.400	0.8389

The Jovanovic isotherm model shares similarities with the Langmuir model, but incorporates an additional possibility of potential mechanical interactions between adsorbate molecules and the adsorbent surface. This

model is particularly effective for predicting of retention capacity of an adsorbent materials under various conditions. The Jovanovic isotherm methodical equation provides the adsorption behavior and capacity of materials with greater precision.

$$\ln q_e = \ln q_m - (K_j) * C_e \quad (11)$$

Where parameters K<sub>j</sub> and q<sub>m</sub> denote the constant of Jovanovic isotherm and maximum adsorbent capacity respectively. Other symbols have the same meaning as in above models. Based on the kinetic theory, the number of active sites increases rapidly with the advancement of adsorption; the Elovich isotherm model is recognized for elucidating multilayer adsorption processes on the adsorbent surface. The linearized Elovich equation elucidates the time-dependent characteristics and dynamic elements of the adsorption process.

$$\ln\left(\frac{q_e}{C_e}\right) = q_m \ln(K_e) - (1/q_m) * q_e \quad (12)$$

The Elovich isotherm constant K<sub>e</sub> is essential for understanding the characteristics of the adsorption process and its underlying mechanisms. The other parameter has same meant as in above models. These variables collectively provide essential insights into the adsorption behavior and equilibrium dynamics of the system.

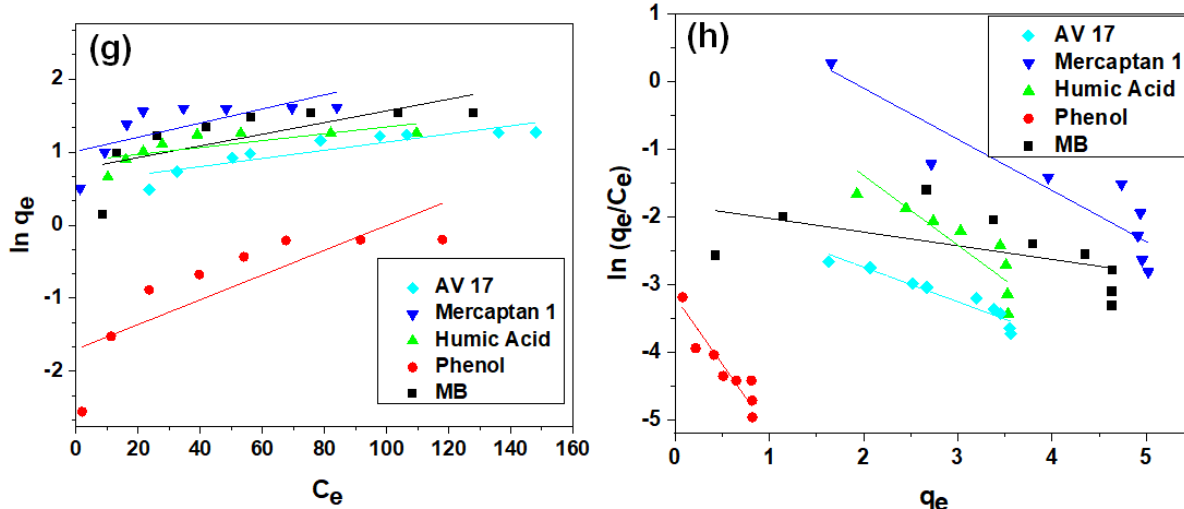


**Figure 6: (g) Jovanovic isotherm and (h) Elovich isotherm models**

The Jovanovic and Elovich isotherm models, illustrating the adsorption behavior for different pollutants were estimated, as shown in Figure 6. The fitting of their experimental data to the both isotherm model is represented in Table. 4. The study of removal of

wastewater pollutants from aqueous solutions by NYEX® 1000 adsorbent. Both isotherms are fit the experimental data are satisfactory due to low correlation coefficient.

**Table 4:** The characteristic values of the kinetics parameter of the models

Pollutants	Jovanovic Isotherm model			Elovich Isotherm model		
Kinetics Characteristic Parameters						
	q <sub>m</sub>	K <sub>j</sub>	R <sup>2</sup>	q <sub>m</sub>	K <sub>e</sub>	R <sup>2</sup>
AV 17	1.780	-6E <sup>-3</sup> 4	0.803	1.990	0.420	0.9136
Marcaptan 1	2.750	-1E <sup>-2</sup> 3	0.512	0.950	1.910	0.8163
Humic acid	2.400	-5E <sup>-3</sup> 8	0.554	1.120	1.260	0.7562
Phenol	0.200	-2E <sup>-2</sup> 9	0.672	0.570	0.030	0.8572
MB	1.220	-2E <sup>-2</sup> 6	0.517	7.420	0.800	0.2023

The selectivity of the 06 adsorption isotherm models for two parameter quantities based on regression coefficient followed the order.

AV 17	Halsey>Temkin>D-R> Elovich> Harkin Jura> Jovanvic
Mercaptan 1	D-R>Elovich>Temkin>Halsey>Harkin Jura>Jovanvic
Humic acid	D-R>Temkin>Halsey>Elovich>Harkin Jura>Jovanvic
Phenol	Halsey>Temkin>Harkin Jura> D-R >Elovich>Jovanvic
MB	D-R>Temkin>Harkin Jura>Halsey>Jovanvic>Elovich

The Halsey isotherm model provided the best match and the most accurate description of the adsorption mechanism of AV 17 and phenol, which was determined to be multilayer. Conversely, it was discovered that the D-R isotherm mechanism led to the adsorption kinetics of Mercaptan 1, Humic acid, and MB, explaining the maximum adsorption capacity of the adsorbent, estimating the characteristics energy of adsorption, and characterizing the strength of contact between the adsorbent and adsorbate.

## Conclusion:

The experimental adsorption kinetics data for different pollutants including AV 17, Mercaptan 1, Humic acid, Phenol and MB on NYEX® 1000, with excellent adsorption performance against several pollutants and electrochemical regeneration were analyzed and compared with kinetic models such as pseudo-first-order and pseudo-second-order kinetics. The numerical calculations of Pseudo-1<sup>st</sup> adsorption kinetics showed its least involvement in adsorption mechanism of all pollutants on surface of NYEX® 1000, revealed through lower regressions values of  $R^2$ . On the contrary, kinetics findings of Pseudo-second order kinetics showed its leading role in adsorption of Humic acid ( $R^2=0.99908$ ), AV 17 ( $R^2=0.9977$ ), Mercaptan ( $R^2=0.9982$ ), Phenol ( $R^2=0.9989$ ) and MB ( $R^2=0.9966$ ) on surface of NYEX® 1000. It confirmed the chemisorption constitutes the rate-limiting phase, indicating a robust interaction

between the adsorbate and the active sites of the adsorbent. The experimental data of adsorption for Mercaptan 1 ( $R^2=0.984$ ), Humic acid ( $R^2=0.9331$ ) and MB ( $R^2=0.9766$ ) on the surface of NYEX® 1000 was found to be well fitted with Dubinin- Radushkevich isotherm model, elucidating the adsorption on microporous materials by positing a pore-filling mechanism based on Gaussian energy distribution and physical adsorption entailing Van Der Waals forces and multilayer development within micropores. Whereas, adsorption calculations for phenol ( $R^2=0.9485$ ) and AV 17 ( $R^2=0.9971$ ) were found in complete agreement with Halsey isotherm model, revealing the multilayer adsorption on heterogeneous porous adsorbents, especially when the adsorbate has been located at a considerable distance from the surface.

## References:

- [1] N. R. Council, "Waste management and control," 1930.
- [2] R. Margaoan *et al.*, "Environmental pollution effect on honey bees and their derived products: A comprehensive analysis," vol. 32, no. 16, pp. 10370-10391, 2025.
- [3] B. Taofeek, O. S. Olukayode, O. I. Samuel, O. J. G. A. R. J. o. E. S. Joshua, and Toxicology, "Hazards of environmental pollution: a global environmental challenges and way forward," vol. 3, no. 1, pp. 1-5, 2014.
- [4] C. Pathak and H. C. J. W. J. o. E. P. Mandalia, IDOSI Publication, UAE, "Impact of environmental pollution on human future," vol. 1, no. 2, pp. 8-10, 2011.
- [5] V. J. W. Saxena, Air, and S. Pollution, "Water quality, air pollution, and climate change: investigating the environmental impacts of industrialization and urbanization," vol. 236, no. 2, p. 73, 2025.
- [6] M. Saleem, T. Pirzada, R. J. C. Qadeer, s. A. physicochemical, and e. aspects, "Sorption of acid violet 17 and direct red 80 dyes on cotton fiber from aqueous solutions," vol. 292, no. 2-3, pp. 246-250, 2007.
- [7] R. O. A. de Lima *et al.*, "Mutagenic and carcinogenic potential of a textile azo dye processing plant effluent that impacts a drinking water source," vol. 626, no. 1-2, pp. 53-60, 2007.

[8] S. Biyada, J. J. C. E. Urbonavičius, and Technology, "Circularity in textile waste: challenges and pathways to sustainability," p. 100905, 2025.

[9] P. Jamshidi and F. J. R. o. C. I. Shemirani, "Adsorption/desorption of acid violet-7 onto magnetic MnO<sub>2</sub> prior to its quantification by UV-visible spectroscopy: Optimized by fractional factorial design," vol. 46, no. 10, pp. 4403-4422, 2020.

[10] N. Roy, S. A. Alex, N. Chandrasekaran, K. Kannabiran, and A. J. J. o. E. M. Mukherjee, "Studies on the removal of acid violet 7 dye from aqueous solutions by green ZnO@ Fe<sub>3</sub>O<sub>4</sub> chitosan-alginate nanocomposite synthesized using *Camellia sinensis* extract," vol. 303, p. 114128, 2022.

[11] R. Sivaraj, C. Namasivayam, and K. J. W. m. Kadirvelu, "Orange peel as an adsorbent in the removal of acid violet 17 (acid dye) from aqueous solutions," vol. 21, no. 1, pp. 105-110, 2001.

[12] Ş. Yalçın Turan, A. Kara, and N. J. I. J. o. E. A. C. Tekin, "Removal of acid violet 7 from aqueous solution with polymer matrix composite particles by adsorption and photocatalytic decolorization methods: isotherms, kinetics, and thermodynamic studies," vol. 105, no. 9, pp. 1996-2021, 2025.

[13] J. W. Fleeger, K. R. Carman, and R. M. Nisbet, "Indirect effects of contaminants in aquatic ecosystems," (in eng), *Sci Total Environ*, vol. 317, no. 1-3, pp. 207-33, Dec 30 2003.

[14] N. S. Gad and A. S. J. G. V. Saad, "Effect of environmental pollution by phenol on some physiological parameters of *Oreochromis niloticus*," vol. 2, no. 6, pp. 312-319, 2008.

[15] A. M. Montebello *et al.*, "Simultaneous methylmercaptan and hydrogen sulfide removal in the desulfurization of biogas in aerobic and anoxic biotrickling filters," vol. 200, pp. 237-246, 2012.

[16] W. E. Luttrell and M. E. Bobo, "Methyl mercaptan," *Journal of Chemical Health & Safety*, vol. 22, no. 5, pp. 37-39, 2015/09/01 2015.

[17] S. Jia *et al.*, "Removal of antibiotics from water in the coexistence of suspended particles and natural organic matters using amino-acid-modified-chitosan flocculants: A combined experimental and theoretical study," vol. 317, pp. 593-601, 2016.

[18] S. Saha and C. J. E. W. Das, "Purification of Humic acids contained simulated wastewater using membrane ultrafiltration," vol. 58, pp. 33-40, 2017.

[19] C. Huang, S. Chen, and J. R. J. W. R. Pan, "Optimal condition for modification of chitosan: a biopolymer for coagulation of colloidal particles," vol. 34, no. 3, pp. 1057-1062, 2000.

[20] Z. L. Yang, B. Y. Gao, Q. Y. Yue, and Y. J. J. o. H. M. Wang, "Effect of pH on the coagulation performance of Al-based coagulants and residual aluminum speciation during the treatment of humic acid-kaolin synthetic water," vol. 178, no. 1-3, pp. 596-603, 2010.

[21] A. Seid-Mohammadi, A. Gh, M. Sammadi, M. Ahmadian, and A. J. R. J. C. E. Poormohammadi, "Removal of humic acid from synthetic water using chitosan as coagulant aid in electrocoagulation process for Al and Fe electrodes," vol. 18, p. 5, 2014.

[22] Y. Pang, Z.-h. Tong, L. Tang, Y.-n. Liu, and K. J. O. C. Luo, "Effect of humic acid on the degradation of methylene blue by peroxymonosulfate," vol. 16, no. 1, pp. 401-406, 2018.

[23] L. Sun, D. Hu, Z. Zhang, X. J. I. J. o. E. R. Deng, and P. Health, "Oxidative degradation of methylene blue via PDS-based advanced oxidation process using natural pyrite," vol. 16, no. 23, p. 4773, 2019.

[24] E. A. Abdelrahman, R. Hegazey, R. E. J. J. o. M. R. El-Azabawy, and Technology, "Efficient removal of methylene blue dye from aqueous media using Fe/Si, Cr/Si, Ni/Si, and Zn/Si amorphous novel adsorbents," vol. 8, no. 6, pp. 5301-5313, 2019.

[25] B. Hameed, I. Tan, and A. L. J. C. e. j. Ahmad, "Adsorption isotherm, kinetic modeling and mechanism of 2, 4, 6-trichlorophenol on coconut husk-based activated carbon," vol. 144, no. 2, pp. 235-244, 2008.

[26] O. M. A. Halim *et al.*, "A review on modified ZnO for the effective degradation of methylene blue and rhodamine B," vol. 18, p. 100408, 2025.

[27] G. Walker and L. J. W. R. Weatherley, "Adsorption of acid dyes on to granular activated carbon in fixed beds," vol. 31, no. 8, pp. 2093-2101, 1997.

[28] A. Bes-Piá, J. Mendoza-Roca, L. Roig-Alcover, A. Iborra-Clar, M. Iborra-Clar, and M. J. D. Alcaina-Miranda, "Comparison between nanofiltration and ozonation of biologically treated textile wastewater for its reuse in the industry," vol. 157, no. 1-3, pp. 81-86, 2003.

[29] T. Robinson, G. McMullan, R. Marchant, and P. J. B. t. Nigam, "Remediation of dyes in textile effluent: a critical review on current treatment technologies with a proposed alternative," vol. 77, no. 3, pp. 247-255, 2001.

[30] V. K. Gupta, I. Ali, V. K. J. J. o. C. Saini, and I. Science, "Adsorption studies on the removal of Vertigo Blue 49 and Orange DNA13 from aqueous solutions using carbon slurry developed from a waste material," vol. 315, no. 1, pp. 87-93, 2007.

[31] P. Ganesan, R. Kamaraj, and S. J. J. o. t. T. I. o. C. E. Vasudevan, "Application of isotherm, kinetic and thermodynamic models for the adsorption of nitrate ions on graphene from aqueous solution," vol. 44, no. 5, pp. 808-814, 2013.

[32] H. S. Rai *et al.*, "Removal of dyes from the effluent of textile and dyestuff manufacturing industry: a review of emerging techniques with reference to biological treatment," vol. 35, no. 3, pp. 219-238, 2005.

[33] S. Azizian and S. Eris, "Chapter 6 - Adsorption isotherms and kinetics," in *Interface Science and Technology*, vol. 33, M. Ghaedi, Ed.: Elsevier, 2021, pp. 445-509.

[34] N. Brown, E. Roberts, A. Garforth, and R. J. E. A. Dryfe, "Electrochemical regeneration of a carbon-based adsorbent loaded with crystal violet dye," vol. 49, no. 20, pp. 3269-3281, 2004.

[35] N. Brown, E. Roberts, A. Chasiotis, T. Cherdron, and N. J. W. r. Sanghrajka, "Atrazine removal using adsorption and electrochemical regeneration," vol. 38, no. 13, pp. 3067-3074, 2004.

[36] F. Mohammed, E. Roberts, A. Hill, A. Campen, and N. J. W. r. Brown, "Continuous water treatment by adsorption and electrochemical regeneration," vol. 45, no. 10, pp. 3065-3074, 2011.

[37] H. M. A. Asghar, *Development of graphitic adsorbents for water treatment using adsorption and electrochemical regeneration*. The University of Manchester (United Kingdom), 2011.

[38] A. K. Bhattacharya and C. J. J. o. E. E. Venkobachar, "Removal of cadmium (II) by low cost adsorbents," vol. 110, no. 1, pp. 110-122, 1984.

[39] S. Shukla and G. J. R. J. o. E. T. Kisku, "Linear and non-linear kinetic modeling for adsorption of disperse dye in batch process," vol. 9, no. 6, p. 320, 2015.

[40] M. Musah *et al.*, "Adsorption kinetics and isotherm models: a review," vol. 4, no. 1, pp. 20-26, 2022.

[41] E. D. Revellame, D. L. Fortela, W. Sharp, R. Hernandez, M. E. J. C. E. Zappi, and Technology, "Adsorption kinetic modeling using pseudo-first order and pseudo-second order rate laws: A review," vol. 1, p. 100032, 2020.